Biological Evaluation of Water Soluble Arene Ru(II) Enantiomers with Amino-Oxime Ligands

Isabel de la Cueva-Alique,[‡] *Sara Sierra,*[‡] *Laura Muñoz-Moreno,*[†] *Adrián Pérez-Redondo,*[‡] *Ana M. Bajo,*[†] *Isabel Marzo,*[⊥] *Lourdes Gude,*[‡] *Tomás Cuenca,*[‡] *Eva Royo*[‡*]

[‡] Departamento de Química Orgánica y Química Inorgánica, Instituto de Investigación Química Andrés M. del Río (IQAR), Universidad de Alcalá, 28805 Alcalá de Henares, Madrid, Spain

[⊥] Departamento de Bioquímica y Biología Molecular y Celular, Universidad de Zaragoza, 50009 Zaragoza, Spain

[†] Departamento de Biología de Sistemas, Facultad de Medicina y Ciencias de la Salud, Universidad de Alcalá, 28805 Alcalá de Henares, Madrid, Spain

Keywords

anticancer, chiral, DNA, in vivo, cytotoxicity, antimetastatic.

Corresponding Author

*E-mail: eva.royo@uah.es. Phone Nr. (+34) 918854629; Fax Nr. (+34) 918854683

ABSTRACT

New water soluble, enantiopure arene ruthenium compound $S_{Ru}S_N$-(1*R*,4*S*)-[(η^6-*p*-cymene)Ru{κNH(Bn),κNOH}Cl]Cl (Bn = benzyl, **1a'**) has been synthesized. The novel compound along with that previously described $R_{Ru}R_N$-(1*S*,4*R*)-[(η^6-*p*-cymene)Ru{κNH(Bn),κNOH}Cl]Cl (**1a**) was evaluated by polarimetry, ultra-violet and circular dichroism spectroscopy. The structure of novel ruthenium derivative **1a'** was determined by single crystal X-ray crystallography. Both enantiomers have been tested against several cancer cell lines *in vitro*: prostate PC-3, lung A-549, pancreas MIA PaCa-2, colorectal HCT-116, leukemia Jurkat and cervical HeLa. Both enantiomers are active and versatile cytotoxic agents, showing IC_{50} values from 2 to 12 times lower than those found for cisplatin in the different cell lines evaluated. The mechanism of cell death induced by the metal compounds was analyzed in A-549 and Jurkat cell lines. Derivatives **1a** and **1a'** induced apoptotic cell death of A-549 cells while dose-dependent cell death mechanisms have been found in the Jurkat cell line. Compound-DNA interactions have been investigated by equilibrium dialysis, Fluorescence Resonance Energy Transfer (FRET) melting assays and viscometric titrations, revealing moderate binding affinity of **1a** and **1a'** towards duplex DNA. Finally, the efficacy of **1a** in a preliminary *in vivo* assay of PC-3 xenografts in nude mice has been evaluated, resulting in a promising inhibition of tumor growth by 45%. Analysis of tumor tissue also showed a significant decrease of levels of crucial molecules in the invasive phenotype of PC-3 cells.

1. Introduction

Although cisplatin and its derivatives are widely used in the clinic, platinum-based compounds possess various problems as anticancer drugs such as high levels of in vivo toxicity, drug resistance and poor aqueous solubility [1]. The development of anti-cancer metal drug candidates to overcome those disadvantages has produced a plethora of possible chemotherapeutics [2-9]. Ruthenium compounds are among the most promising candidates with currently KP1339 (sodium *trans*-[tetrachloridobis(1H-indazole)-ruthenate(III)]) and NAMI-A (imidazolium *trans*-[tetrachloridobis(dimethylsulfoxide)(1H-imidazole)-ruthenate(III)]) having entered clinical trials [8,10-13]. Another promising class of antitumor ruthenium-based compounds are the arene ruthenium RAPTA derivatives, with RAPTA-C ([(η^6-*p*-cymene)Ru(pta)Cl_2], pta = 1,3,5-triaza-7-phosphatricyclo[3.3.1]decane) in advanced pre-clinical studies [14,15].

The effect of stereochemistry on biological activity is of great importance in medicinal chemistry, as many of the biological targets are chiral [16-20]. About more than half of the drugs currently in clinical use are chiral compounds, marketed as racemates or as single enantiomers. The anticancer properties of chiral metal derivatives have been largely explored [21-36], but the role of the stereochemistry in the biological activity of non-platinum based compounds has been less investigated [18-20,37-48]. From those enantiomers isolated and studied, different antitumor activities by factors of 2-6 have been found for ruthenium [19,37,41,44,48], osmium [20], and titanium [17,40,45,46] compounds. Thus, Manna et al [17] proposed that stereochemistry should be considered in the design, modification, and improvement of active compounds.

Oxime groups offer significant advantages for biological application. They possess stronger hydrogen–bonding abilities than alcohols or carboxylic acids and thus, they can

favor solubility of the resulting compounds in biological media [49]. In addition, some oxime organic derivatives have been reported to have anticancer properties [50,51]. Oxime-containing Pt(II), Rh(III), Ir(III) and Ru(II) compounds with antitumoral properties reported to date have shown strong anticancer activities whereas the compounds do not interact with DNA in a similar way to cisplatin [52-57]. This fact opens the gate to the discovering of therapeutic anticancer drugs with different mechanisms of action than those of cisplatin and derivatives [58,59].

Studies of enantiopure arene ruthenium anticancer derivatives are scarce [19,20,48], probably due to the difficult isolation of unique stereoisomers of such organometallic compounds [22,60]. Recently, a Noyori-like arene Ru(II) catalyst have shown a broad range of potent anticancer activities [48]. Other enantiopure, chiral-at-metal arene group 8 compounds that have demonstrated high cytotoxic profiles are the Os(II) iminopyridine halide enantiomers of general formula [{(η^6-*p*-cymene)Os(ImpyMe)I]PF_6 (ImpyMe = N-(2-pyridylmethylene)-1-phenylethylamine) [20]. Optically active RAPTA analogues have been also studied showing good cytotoxic potency against human ovarian carcinoma A-278 cells [19].

We have recently reported an optically active *p*-cymene ruthenium(II) compound with an amino-oxime ligand derived from *R*-limonene, of formula $R_{Ru}R_N$-(1*S*,4*R*)-[(η^6-*p*-cymene)Ru{κNH(Bn),κNOH}Cl]Cl (Bn = benzyl, **1a**) (Fig. 1), which possess relevant antitumor properties. Our compound shows high solubility in water and significant effects on cytotoxicity, cell adhesion to collagen and migration of androgen-independent prostate PC-3 cancer cells while it does not seem to exhibit strong interactions with plasmid DNA by electrophoretic mobility shift assays and Calf Thymus (CT) DNA thermal denaturing experiments [61].

FIGURE 1

Encouraged by our previous results, we decided to explore the reactions of [(η^6-*p*-cymene)$RuCl_2]_2$ with the amino-oxime chiral organic compound (1*R*,4*S*)-{NOH,(Bn)NH} (**a'**, see Fig. 2) [62,63], derived from *S*-limonene. This naturally occurring terpene is an inexpensive starting reagent, commercially available in an optically pure form and easily tailored by stereoselective functionalization [64,65].

We report here on the synthesis and characterization of the novel Ru(II) enantiomer $S_{Ru}S_N$-(1*R*,4*S*)-[(η^6-*p*-cymene)Ru{κNH(Bn),κNOH}Cl]Cl (**1a'**). The new compound along with that previously described, **1a**, have been evaluated against several cancer cell lines *in vitro*: prostate PC-3, lung A-549, pancreas MIA PaCa-2, colorectal HCT-116, leukemia Jurkat and cervical HeLa. The mechanism of cell death induced by these ruthenium complexes was analyzed in A-549 and Jurkat cell lines. DNA interactions of both enantiomers have been investigated by Fluorescence Resonance Energy Transfer (FRET) melting assays, dialysis and viscometric titrations experiments. Additionally, we describe the efficacy of **1a** in an *in vivo* evaluation of PC-3 xenografts in nude mice.

2. Experimental Section

2.1. Chemicals and synthesis

Synthesis of ruthenium complexes **1a** and **1a'** were performed without exclusion of moisture or air. Solvents were dried by known procedures and used freshly distilled. (1*S*,4*R*)-, (1*R*,4*S*)-[NH(Bn),NOH] (**a**, **a'**) and corresponding adducts (1*S*,4*R*)-, (1*R*,4*S*)-[NH(Bn)·HCl,NOH] (**a·HCl**, **a'·HCl**) were prepared according to previous reports [62,63,66,67]. *R*- or *S*-limonene and isopentyl nitrite were reacted following the standard method described by Carman et al in 1977 [66]. *R*-limonene, *S*-limonene, [(η^6-*p*-cymene)$RuCl_2]_2$, and cisplatin (*cis*-$[PtCl_2(NH_3)_2]$) were purchased from Sigma-Aldrich. Commercially available reagents were used without further purification.

Nuclear Magnetic Resonance (NMR) spectra were recorded on a Bruker 400 Ultrashield. ^{1}H and ^{13}C chemical shifts are reported relative to tetramethylsilane. ^{15}N chemical shifts are reported relative to liquid ammonia (25 ºC). Coupling constants *J* are given in Hertz. Elemental analysis was performed on a LECO CHNS 932 Analyzer at the Universidad de Alcalá or, alternatively, at the Universidad Autónoma de Madrid. Infrared (IR) spectra were recorded on IR Fourier Transform (FT) Perkin Elmer (Spectrum 2000) spectrophotometer on KBr pellets. The pH was measured in a HANNA HI208 pHmeter in distilled water solutions. Circular Dichroism (CD) spectra were recorded on a J-715 CD spectropolarimeter (Jasco, UK) at ambient temperature (297 K). The spectra were determined at a concentration of 0.5 mM in water using a quartz cuvette of 0.5 cm path length, scan speed of 20 $nm \cdot min^{-1}$, 0.1 nm band width, 0.5 nm data pitch and 0.5 s of response time. Optical rotations of all the compounds solutions were recorded on a Perkin Elmer 341 polarimeter, using the sodium D line (589 nm) at ambient temperature (297 K) in a quartz cell of 1 dm path length. Specific optical rotation values were calculated according to the equation $[\alpha]^{24}_{D} = 100 \cdot \alpha_{obs}/l \cdot c$ [68]. Analytical balance and volumetric pipettes (2.0 mL) were used to prepare $CHCl_3$ solutions of the compounds at concentrations within a range of 7.50-7.80 $g \cdot mL^{-1}$. Ultra-violet visible (UV-vis) spectra were measured at room temperature on water solutions of the compounds with a Perkin Elmer Lambda 35 spectrophotometer.

2.1.1. $S_{Ru}S_{N}$-*(1R,4S)*-[(η^6-*p*-cymene)Ru{kNH(Bn),kNOH}Cl]Cl (**1a'**). An analogous procedure to that described before for the synthesis of **1a** [61,67] was used. A dichloromethane (10 mL) solution of **a'** (0.27 g, 0.98 mmol) and [(η^6-*p*-cymene)$RuCl_2$]$_2$ (0.30 g, 0.49 mmol) was stirred for 30 min at room temperature. Evaporation of the solvent affords a yellow solid. Yield: 0.25 g (83%). $[\alpha]^{23}_{D}$ ($deg \cdot dm^{-1} \cdot dL \cdot g^{-1}$) -94.2 ± 1.2 (**1a'** at c = 0.764 $g \cdot dL^{-1}$, α_{obs} = -0.720 deg), +94.3 ± 1.2 (**1a** at c = 0.764 $g \cdot mL^{-1}$, α_{obs} =

+0.721 deg). Solubility in H_2O at 24 ºC (mM): 28 ± 4 mM. Value of pH ([9.0 mM]) in H_2O at 24 ºC: 4.70. Analytical and spectroscopic data of the compound are identical to those reported before [61,67] (see Supplementary data). Anal. Calcd for $C_{27}H_{38}Cl_2N_2ORu$: C, 56.05; H, 6.62; N, 4.84; Found: C, 55.78; H, 6.57; N, 5.15. IR (KBr, λmax/cm^{-1}): 3400-3040 ν(NH/NOH), 1643, 1600 ν(C=N). UV-vis (0.1 mM in H_2O): λmax (ε): 246 (8111), 324 (1577), 422 (631). Since NMR spectra of the compound in chloroform-d_1 changed dramatically within a concentration range of ca. 5-62 mM, full characterization was carried out in methanol-d_4 [61]. ^{1}H NMR (plus HSQC, plus HMBC, 400.1 MHz, 293 K, methanol-d_4): δ 7.45 (m, overlapped, C_6H_5), 5.85, 5.84, 5.46, 5.33 (all d, each 1 H, J_{HH} = 3, *p*-cymene-C_6H_4), 4.79 (s, 1H, =CH_2), 4.72 (second order system, 2H, -CH_2), 4.60 (s, 1H, =CH_2), 4.02 (br, 1H, NH), 3.60 (d, 1H, J_{HH} = 16, -CH_2^3), 2.53 (overlapped, 3H, *p*-cymene-$CHMe_2$ + -CH^4 + -CH_2^3), 2.14 (m, 1H, -CH_2^6), 1.99 (s, 3H, *p*-cymene-CH_3), 1.83 (m, 2H, -CH_2^5), 1.66, 1.65 (both s, each 3H, $CqCH_3$ +CH_3-C=), 1.39 (m, 1H, -CH_2^6), 1.22, 1.02 (both d, each 3H, J_{HH} = 6, *p*-cymene-CH(CH_3)$_2$). ^{13}C NMR (plus Attached Proton Test (APT), plus gradient Heteronuclear Single Quantum Coherence (gHSQC), plus Heteronuclear Multiple Bond Correlation (HMBC), 100.6 MHz, 293 K, methanol-d_4): δ 170.8 (−, Cq=N), 145.9 (−, =*Cq*-Me), 137.1 (−,C_{ipso} -C_6H_5), 130.1, 129.5, 129.4 (all +, -C_6H_5), 113.2 (−, =CH_2), 108.9, 98.8 (both −, C_{ipso}-*p*-cymene), 87.5, 84.8, 83.3, 83.2 (all +, *p*-cymene:C_6H_4), 70.5 (−, Cq-NH), 55.9 (−, -CH_2Ph), 39.4 (+, -CH^4), 35.4 (−, -CH_2^6), 32.5 (+, *p*-cymene-$CHMe_2$), 29.1 (−, -CH_2^3), 25.1 (−, -CH_2^5), 23.9 (+, *p*-cymene-CH(CH_3)$_2$), 22.3 (+, CH_3-CNH), 20.8 (+, *p*-cymene-CH(CH_3)$_2$), 20.7 (+, CH_3-C=), 18.4 (+, CH_3-:*p*-cymene). ^{15}N NMR (gHMBC, 40.5 MHz, 293 K, chloroform-d_1): δ 272.0 (C=N), 50.4 (NHBn). ^{15}N NMR (gHMBC, 40.5 MHz, 293 K, methanol-d_4): δ 266.7 (C=N), 50.0 (NHBn).

2.1.2. ^{1}H NMR experiments at physiological pH. Phosphate buffered saline solution (PBS) was prepared according to Cold Spring Harbor Protocols (http://cshprotocols.cshlp.org/content/2006/1/pdb.rec8247) using NaCl, KCl, Na_2HPO_4 and KH_2PO_4 in D_2O. Adjustment of pD (pD = pH* + 0.4, where pH* = pHmeter reading in D_2O) was carried out using a solution of DCl (0.01M) or NaOD (0.01M) in D_2O, with the help of a HANNA HI208 pHmeter..

2.2. Single-crystal X-ray structure determination

Yellow crystals of the pure enantiomer **1a'**·$2CHCl_3$ were grown from a hexane-chloroform solution. The crystals were removed from the vial and covered with a layer of a viscous perfluoropolyether. A suitable crystal was selected with the aid of a microscope, mounted on a cryo-loop, and placed in the low-temperature nitrogen stream of the diffractometer. The intensity data sets were collected at 200 K on a Bruker-Nonius Kappa CCD diffractometer equipped with an Oxford Cryostream 700 unit. The molybdenum radiation (λ = 0.71073) was used, graphite monochromated, and enhanced with an MIRACOL collimator.

The structure was solved, using WINGX package [69], by intrinsic phasing methods (SHELXT) [70], and refined by least-squares against F^2 (SHELXL-2014/7) [70]. Crystals of **1a'** contained two independent molecules in the asymmetric unit, but there were no significant differences between them. **1a'** crystallized with two molecules of chloroform per ionic pair. All non-hydrogen atoms were anisotropically refined, whereas the hydrogen atoms were included, positioned geometrically, and refined by using a riding model. DELU and SIMU restraints were used for the aromatic ring C(32)-C(37) of a benzyl group. *Crystal data for* **1a'**·$2CHCl_3$: ($C_{29}H_{40}Cl_8N_2ORu$), FW = 817.30, Monoclinic, space group $P2_1$, crystal dimensions (mm^3) 0.31 x 0.13 x 0.12, a = 8.865(2), b = 21.916(2), β = 90.49(1), c = 18.183(2) Å, V = 3532.7(8) $Å^3$, Z = 4, ρ_{calcd} =

1.537 g cm^{-3}, μ = 1.075 mm^{-1}, F(000) = 1664, θ range = 3.00 to 25.24 deg, no. of rflns collected = 66843, no. of indep rflns / R_{int} = 12759 / 0.174, no. of data / restraints / params = 12759 / 49 / 751, *R*1 / *wR*2 ($I>2\sigma(I)$) = 0.071 / 0.114, *R*1 / *wR*2 (all data) = 0.132 / 0.134, GOF (on F^2) = 1.085, Absolute structure parameter = –0.06(2). Final difference Fourier maps did not show peaks higher than 0.699 nor deeper than –0.588 $eÅ^{-3}$. CCDC-1572919 contains the supplementary crystallographic data for this paper. These data can be obtained free of charge from The Cambridge Crystallographic Data Centre via www.ccdc.cam.ac.uk/structures.

2.3. Cell culture, cytotoxicity assays and cell death analysis

2.3.1. Cell culture

The androgen-unresponsive prostate cancer cell line PC-3 was obtained from the American Type Culture Collection (Manassas, VA) and may be related to recurrent prostate cancers that have achieved androgen independence. All culture media were supplemented with 1% penicillin/streptomycin/amphoterycin B (Life Technologies, Barcelona, Spain). The culture was performed in a humidified 5% CO_2 environment at 37 °C. After the cells reached 70–80% confluence, they were washed with PBS, detached with 0.25% trypsin/0.2% ethylendiaminetetraacetic acid (EDTA) and seeded at 30,000–40,000 cells·cm^{-2}. The culture medium was changed every 3 days. A-549 (lung carcinoma) cells were maintained in high glucose DMEM (Dulbecco´s Modified Eagle´s Medium) supplemented with 5% fetal bovine serum (FBS), 200 U·mL^{-1} penicillin, 100 µg·mL^{-1} streptomycin and 2 mM L-glutamine. MIA PaCa-2 (pancreas carcinoma), HCT-116 (colorectal carcinoma), HeLa (cervical cancer), Jurkat (leukemic cancer), Jurkat-pLVTHM (obtained by transfection with nonspecific short hairpin ribonucleic acid (shRNA)) and Jurkat-shBak (obtained by ribonucleic acid interference (RNAi) of Bak) cells were maintained in Roswell Park Memorial Institute (RPMI) 1640

medium supplemented with 5% FBS, 200 $U \cdot mL^{-1}$ penicillin, 100 $\mu g \cdot mL^{-1}$ streptomycin and 2 mM L-glutamine. Cultures were maintained in a humidified atmosphere of 95% air:5% CO_2 at 37 °C. Adherent cells were allowed to attach for 24 h prior to addition of compounds.

2.3.2. MTT Toxicity Assays

For toxicity assays, cells (5×10^4 for Jurkat cells and 10^4 for adherent cell lines) were seeded in flat-bottom 96-well plates (100 µL/well) in complete medium. Adherent cells were allowed to attach for 24 h prior to addition of cisplatin or tested compounds. Stock solutions of ammonium-oxime pro-ligands were freshly prepared in 1% of dimethyl sulfoxide (DMSO) in water, while cisplatin and *p*-cymene ruthenium compounds were dissolved in water. The stock solutions were then diluted in complete medium and used for sequential dilutions to desired concentrations. The final concentration of DMSO in the cell culture medium did not exceed 0.1%. Control groups with and without DMSO (0.1%) were included in the assays. Compounds were then added at different concentrations in quadruplicate. Cells were incubated with compounds for 24 h, and then cell proliferation was determined by a modification of the MTT-reduction method. Briefly, 10 µL/well of [3-(4,5-dimethylthiazol-2-yl)-2,5-diphenyltetrazolium bromide] (MTT) (5 $mg \cdot mL^{-1}$ in PBS) was added, and plates were incubated for 1−3 h at 37 °C. Finally, formazan crystals were dissolved by adding 100 µL/well *iso*-propanol (0.05 M HCl) and gently shaking. The optical density was measured at 550 nm using a 96-well multi-scanner auto-reader (Enzyme-Linked Inmuno Sorbent Assay, ELISA).

2.3.3. Cell Death Analysis

Apoptosis hallmarks of cells treated with the metal compounds were analyzed by measuring the exposure of phosphatidylserine. Cells were treated with the compound at 2.5 µM for 24 h and phosphatidylserine exposure was quantified by labeling cells with

annexin V-DY634 (Invitrogen). Annexin V was added at a concentration of 0.5 $\mu g \cdot mL^{-1}$ in Annexin Binding Buffer (ABB), and cells were incubated at room temperature for 15 min. Finally, cells were diluted to 500 μL with ABB to be analyzed by flow cytometry (FACScan, BD Bioscience, Spain). Cell morphology after treatment with metal compounds was evaluated through optical microscopy.

2.4. DNA interaction studies

2.4.1. Equilibrium Dialysis

Duplex DNA from CT (Deoxyribonucleic acid, Activated, Type XV) was directly purchased from Sigma Aldrich and used as provided. Duplex-forming oligonucleotides ds17-1 (5'-CCA GTT CGT AGT AAC CC-3') and ds17-2 (5'-GGG TTA CTA CGA ACT GG-3') were acquired High Performance Liquid Chromatography (HPLC) purified and desalted from Integrated DNA Technologies (IDT). Dialysis membranes (Spectra/Por® molecular porous membrane tubing MWCO: 3.5–5.0 kDa; 6.4 mm diameter) were purchased from Spectrum Laboratories Inc. Aqueous solutions of surfactant sodium dodecyl sulfate (10%) were purchased from Sigma Aldrich. The buffer employed in this experiment was 10 mM phosphate buffer NaH_2PO_4/Na_2HPO_4, pH = 7.2, with either 10 mM or 100 mM NaCl. The solutions of DNA were prepared in the working phosphate buffer at 75 μM monomeric unit (m.u.) concentrations, in base pairs. For the preparation of the short oligonucleotide solution, an annealing step was needed, with heating at 90 °C for 10 min and then gradually cooling to 25 °C during 3 h. The solutions were left at 4 °C overnight.

Dialysis bags, previously washed with milli-Q water, were filled with 75 μM (m.u.) of DNA duplex (200 μL each bag) and placed in a beaker containing 225 mL of ca. 20 μM solution of the tested compound. The beaker was covered with parafilm and aluminium foil and allowed to equilibrate during 24 h at room temperature. Experiments

were run, at least, in triplicate. Once the dialysis process had been completed, the solutions from each dialysis bag were transferred to Eppendorf tubes. The content of each bag was then mixed with an aqueous detergent solution (10%) to reach a 1% concentration (v/v) of sodium dodecyl sulfate (SDS). The concentrations of free compound in the dialysate solution and compound in the dialysis bags were determined by absorbance measurements using the extinction coefficients of the metal complexes (determined in the presence and absence of the detergent) and apparent association constants were calculated [71].

2.4.2. DNA FRET melting assay

The DNA melting assay was performed on a quantitative PCR kit ABI PRISM® 7000 Sequence Detection System (Applied Biosystems) in a 96-well plate format (96-Well Optical MicroAmp® Reaction Plate, Applied Biosystems, Life Technologies Corporation). The oligonucleotide sequence employed in this experiment, F10T (5'-FAM-AGC TAT TA TA /sp18/ TA TA GCT ATA-TAMRA-3') was produced, HPLC-purified and desalted by IDT. FAM is 6-carboxyfluorescein and TAMRA is carboxytetramethylrhodamine. The buffer system used in this experiment was: 10 mM sodium cacodylate, 100 mM LiCl, (pH = 7.3). First, the duplex-forming oligonucleotide was dissolved in water (Biotechnology Performance Certified, BPC grade) and a 50 μM stock solution was prepared, which was then diluted to 0.5 μM. Then, the diluted DNA solution was mixed with the working buffer (2x) and water (BPC grade). The DNA solution was heated at 90 °C for 10 min, cooled down slowly for 3 h and left at 4 ºC overnight. Compounds to be tested were dissolved in water and approximately 1 mM stock solutions were prepared. The exact concentrations were checked by UV-vis. Stock solutions were then diluted with buffer to obtain 50 μM solutions of each compound. In a 96-well microplate, DNA solutions were mixed with solutions of tested compound

and buffer to reach a total volume of 50 μL with a F10T concentration of 0.2 μM and a compound concentration ranging between 1 and 10 μM.

The experimental protocol consisted of an incubation for 5 min at 24 °C, followed by a temperature ramp with heating rate 1 °C/min. Fluorescence values corresponding to the fluorophore FAM at wavelength of 516 nm (after excitation at 492 nm) were collected at each degree of temperature. Afterwards, the fluorescence data were normalized, plotted against temperature (ºC) at each compound concentration, and melting temperatures (T_m) values were determined.

2.4.3. Viscometric titrations

Duplex DNA from CT (Deoxyribonucleic acid, Activated, Type XV) was purchased from Sigma Aldrich and used as provided. The buffer employed in this experiment was 10 mM phosphate buffer NaH_2PO_4/Na_2HPO_4, pH = 7.2. The viscosimetric measurements were performed in a Visco System AVS 470 at 25.00 ± 0.01 ºC, using a microUbbelohde (K = 0.01) capillary viscometer. 6 mL of DNA solution (0.4 mM in nucleotides) in phosphate buffer were equilibrated for 20 min at 25.00 ºC and then 20 flow times were registered. Small aliquots (30–50 μL) of solutions of metal complexes (1.6–2.3 mM) were added to the same DNA solution. Before each flow time registration, the solutions were equilibrated for 20 min to 25.00 ºC and then 20 flow times were measured. With the averaged time of the different flow time measurements and the viscometer constant, the viscosities (μ) for each point were calculated. The viscosity results were plotted as $(\mu/\mu_0)^{1/3}$, where μ_0 represents the DNA solution viscosity in the absence of the ligand, versus (r), representing the ratio [ligand]/[DNA].

2.5. *In vivo* Test

2.5.1. Animals, xenografts, and processing of tumors

Athymic male nude mice (nu/nu) 4 weeks old were obtained from Harlan (Oxon, UK) and maintained in microisolator units on a standard sterilizable diet. Mice were housed under humidity- and temperature-controlled conditions, and the light/dark cycle was set at 12 h intervals. Experimental procedures are carried out according to Spanish Law 32/2007, Spanish Royal Decree 1201/2005, European Directive 609/86/CEE and European Convention of Council of Europe ETS 123. PC-3 cells were incubated in the absence or presence of 2.5 μM **1a** for 24 h. Then, they were washed with PBS, detached with 25% trypsin/0.2% EDTA, centrifuged at 400 × g, and re-suspended in fresh medium at 1×10^8 cells/mL. The cell suspension was mixed with Matrigel® (BD Bioscience) synthetic basement membrane (1:1, v/v) and then injected subcutaneously into the right flank of nude mice (5×10^6 cells/mouse). Ten animals were used per group. Tumors were harvested after sacrifice at 6 weeks of subcutaneous cell injection. Animals were divided into two groups: group 1, control; group 2, **1a**. Tumor volume (mm^3) = (length × width × height × 0.5236) was assessed every three or four days. The experiment was ended on day 43. All mice were euthanized by cervical dislocation upon study completion and tumors collected postmortem. Tumor specimens were frozen in liquid nitrogen and maintained at −80°C for further experiments.

2.5.2. Isolation of tissue lysates

Tumor specimens were homogenized in 50 mM Tris–HCl (pH 7.6) containing 1% Triton X-100, 200 mM NaCl, 10 mM $CaCl_2$, 5 $\mu g \cdot mL^{-1}$ aprotinin, 5 $\mu g \cdot mL^{-1}$ leupeptin, and 5 $\mu g \cdot mL^{-1}$ pepstatin and then rotated for 30 min in a cold room. The extract was cleared by centrifugation at 15,000 × g for 30 min at 4 °C.

2.5.3. Determination of Vascular Endothelial Growth Factor (VEGF)

VEGF levels were determined in tumor homogenates (25 μg) by ELISA, (human VEGF DuoSet, R&D Systems, Madrid, Spain) according to the manufacturer's instructions. Data were normalized to the protein concentration in each sample. *Gelatin zymography:* The tumor homogenates were analyzed by zymography using 10% sodium dodecyl sulfate polyacrylamide gel electrophoresis (SDS–PAGE) containing 0.1% (w/v) gelatin (Sigma, Alcobendas, Spain) as the substrate. Each lane was loaded with a 3 μg protein and subjected to electrophoresis at 4 ºC. Gels were washed twice in 50 mM Tris (tris(hydroxymethyl)aminomethane, pH 7.4) containing 2.5% (v/v) Triton X-100 for 1 h, followed by two 10-min rinses in 50 mM Tris (pH 7.4). After SDS removal, gels were incubated overnight in 50 mM Tris (pH 7.5) containing 10 mM $CaCl_2$, 0.15 M NaCl, 0.1% (v/v) Triton X-100, and 0.02% sodium azide at 37 ºC under constant shaking. Then, gels were stained with 0.25% Coomasie Brilliant Blue R-250 (Sigma) and distained in 7.5% acetic acid with 20% methanol. MMP-2 (metaloproteinase-2) and MMP-9 (metaloproteinase-9) activities were semiquantitatively determined by densitometry.

2.5.4. Data analysis

Results were subjected to computer-assisted statistical analysis using One-Way Analysis of Variance ANOVA, Bonferroni´s post-test, and Student´s t-test. Data are shown as the means of individual experiments and presented as the mean ± SD (Standard deviation). Differences of $P < 0.05$ were considered to be significantly different from the controls.

3. Results and Discussion

3.1. Synthesis and characterization of metal compounds

Synthesis of the novel Ru(II) compound was carried out analogously to that of previously described enantiomer **1a** [61,67]. Thus, the reaction of dimer [(η^6-*p*-cymene)$RuCl_2$]$_2$ with amino-oxime derivative (1*R*,4*S*)-{NOH,(Bn)NH} (**a'**), proceeds also stereoselectively to afford enantiomerically pure $S_{Ru}S_N$-(1*R*,4*S*)-[(η^6-*p*-cymene)Ru{κNH(Bn),κNOH}Cl]Cl (**1a'**) (Fig. 2).

FIGURE 2

Since Ru(II) compound **1a'** is a chiral-at-metal complex with a new stereogenic centre at the amino ligand, four different diastereomers distinguishable by NMR spectroscopy could be formed, namely $R_{Ru}S_N$-(1*R*,4*S*)-, $R_{Ru}R_N$-(1*R*,4*S*)-, $S_{Ru}S_N$-(1*R*,4*S*)- or $S_{Ru}R_N$-(1*R*,4*S*)-**1a'**. ^{1}H and ^{13}C NMR spectra of the solid showed the existence of only one diastereomer in solution, which has been fully characterized as $S_{Ru}S_N$-(1*R*,4*S*)-[(η^6-*p*-cymene)Ru{κNH(Bn),κNOH}Cl]Cl (**1a'**). Epimerization [22,60,72,73] was never observed in chloroform-d_1, acetone-d_6, methanol-d_4, water-d_2 or PBS solutions over time (up to 72 h), within a temperature range of 10-60 ºC (see Supplementary data, Fig. S4, S5, S6, S9), suggesting a preferred mode of the ligand chelation [74-79]. Similar results had previously been observed by us during the synthesis and characterization of derivative **1a** [61].

Analytical and spectroscopic data of the novel compound **1a'** are identical to those reported before for **1a** [61,67] (see Experimental Section and Fig. S3-S9, S11). The UV-vis spectrum of **1a** or **1a'** (see Supplementary data, Fig S11) shows two absorption bands at 324 and 422 nm, followed by a more intense band at 246 nm. Both derivatives gave complementary CD spectra (Fig. 3), with opposite Cotton effects at 246, 284, 320 and 380 nm. Although CD cannot give information on the absolute configuration, these results confirm that the molecular structures of **1a** and **1a'** are mirror images [20].

FIGURE 3

Calculated data of specific optical rotation in chloroform solution for the pro-ligands and metal compounds ($[\alpha]^{23}_{D}$ ($deg \cdot dm^{-1} \cdot dL \cdot g^{-1}$) = +130 ± 1.3 **a**, -127 ± 1.3 **a'**, +94.3 ± 1.2**1a**, -94.2 ± 1.2 **1a'**) evidence again the enantiomeric relationship of the stereoisomers. Furthermore, absolute configuration of compound **1a'** has been confirmed through X-ray structure determination (Fig. 4, Table S1, S2, Fig. S13). X-ray molecular structure of **1a** was reported elsewhere [67].

The solid-state structure of **1a'** contains two independent molecules in the asymmetric unit, with no substantial differences between them (Table S2), and with the same absolute configuration of the four chiral centers. An ORTEP diagram of one of these independent molecules is shown in Fig. 4. The compound adopts the expected piano-stool geometry, with the ruthenium atom bound to the arene ligand through η^6 bonding. All the bond lengths and angles are in agreement with analogous oxime ruthenium compounds previously reported [56,57,67,80].

FIGURE 4

3.2. *In vitro* cell studies

3.2.1. Anti-proliferative studies

Chiral compound **1a** has already shown their promising anticancer properties on the human prostate cancer cell line PC-3 [61].

Epimerization at the Ru(II) center of **1a** or **1a'** after a 72 h incubation period under physiologically relevant conditions does not occur (Fig. S9). This fact suggests that the complexes are stable enough to allow further investigations into the effect of chirality on their anti-proliferative effectiveness. Thus, in order to compare and evaluate the

versatility of the different enantiomers, the cytotoxic activity of pro-ligands **a·HCl** and **a'·HCl** and metal compounds $[(\eta^6\text{-}p\text{-cymene})RuCl_2]_2$, **1a** and **1a'** was now assessed on a wide variety of human cancer cell lines, i.e. prostate PC-3, lung A-549, pancreas MIA PaCa-2, colon HCT-116, leukemia Jurkat-T, and cervical HeLa. The *in vitro* effect of the compounds on cytotoxicity was evaluated by monitoring their ability to inhibit cell growth using the MTT assay after 24 h of incubation time.

While pro-ligands **a·HCl**, **a'·HCl** and metal compound $[(\eta^6\text{-}p\text{-cymene})RuCl_2]_2$ are poorly cytotoxic in all tested cell lines (IC_{50} > 150 μM under this experimental conditions), both enantiomers **1a** and **1a'** are versatile cytotoxic agents, with IC_{50} values ranging from 4.0 to 18.4 μM in the different cell lines tested (Table 1).

TABLE 1

These ruthenium compounds showed better cytotoxic profiles than those found for cisplatin (from 2 to 12 times more active), with only minor differences observed between the two enantiomers.

Our compound, with an IC_{50} value of 7.2 μM, is as cytotoxic in lung cancer A-549 cells as the promising iminophosphorane Ru(II) compound $[(\eta^6\text{-}p\text{-cymene})Ru(Ph_3P{=}NCO\text{-}2\text{-}NC_5H_4\text{-}\kappa N,O)Cl]Cl$ (IC_{50} = 9.5 μM, 24 h) [81]. **1a** is also as active as Sadler's compound $[(\eta^6\text{-}C_6H_5Ph)Ru(en)Cl][PF_6]$ (RM175, en = ethylenediamine) in colon carcinoma HCT-116 cells (IC_{50} = 16 μM) [82]. A highly efficient ruthenium complex against colorectal cancer cells is the cyclopentadienyl Ru(II) carbohydrate containing compound described by Florindo et al (IC_{50} values of 0.45 μM in HCT-116 cells, 72 h, as potent as oxaliplatin ([Pt(oxalate)(*R*,*R*-1,2-diaminocyclohexane)]), the first choice of treatment for colon carcinoma patients in advanced stages [83]). Other promising Ru(II) compounds are the cyclopentadienyl ciprofloxacin derivate reported by Ude et al [84], with IC_{50} values after 24 h of exposure to the drug as low as 0.25 μM (A-549), 1.33

(HCT-116) and 1.46 (PC-3) and the 2,2'-bypyridine derivative [(η^5-C_5H_5)Ru(bypy)(PPh_3)][CF_3SO_3] (TM34, IC_{50} = 0.54 in PC-3 cells, 72 h) [85].

3.2.2. Mechanism of cell death

The mechanism of cell death induced by these chiral oxime compounds was analyzed in A-549 and Jurkat cell lines.

Cell morphology evaluation of A-549 cells indicated that ruthenium derivatives **1a** and **1a'** induced apoptotic cell death, characterized by condensed nuclei and membrane blebbing. Cis-platin was included in the experiment as a positive control, since cisplatin-treated cells show typical apoptotic morphology (Fig. S14).

We analyzed the implication of mitochondria in the toxicity of metal compounds. In the intrinsic pathway of apoptosis, initiated by cell damage, the pro-apoptotic Bax and Bak proteins are required for the release of cytochrome C from mitochondria. Thus, cells lacking these two proteins cannot activate the intrinsic pathway and are usually resistant to chemotherapy drugs. Jurkat cells do not express Bax, due to a genetic deletion, and the subline Jurkat-shBak cells, obtained by RNAi of Bak [86], are deficient in both proteins. Thus, Jurkat-shBak cell line constitutes a model of human leukemia cells deficient in the intrinsic (mitochondrial) pathway of apoptosis. A cell line transfected with a nonspecific shRNA (named Jurkat pLVTHM) was used as a control in these experiments, to discard any unspecific effect due to the transfection and selection process necessary to generate the Jurkat shBak subline.

A comparison between the effect of **1a** and starting materials on Jurkat-T cell apoptosis has been performed. As shown in Fig. 5, **1a** (2.5 μM), but not the starting materials **a·HCl** (5 μM), [(η^6-*p*-cymene)$RuCl_2$]$_2$ (2,5 μM), or the combined dose of both, induced cell death in a high percentage of Jurkat control (pLVTHM) cells but not

in Jurkat-shBak cells, suggesting that, **1a** induced cell death through the intrinsic pathway at these concentrations.

FIGURE 5

Dose-response experiments using the MTT assay (Fig. S15) showed that both enantiomers **1a** and **1a'** exhibited toxicity at concentrations higher than 10 μM in both Jurkat cell lines, suggesting that Bax/Bak-independent cell death mechanisms can be also activated by these compounds. DNA interaction analysis described below revealed that the two enantiomers partially bind to DNA. In a cellular context, this interaction with DNA could likely induce DNA damage and activation of the intrinsic pathway of apoptosis. Interestingly, at higher doses both compounds can circumvent the lack of Bax and Bak, indicating that apoptosis-resistant tumors that are commonly resistant to chemotherapy could be sensitive to them through alternative cell death mechanisms.

3.3. DNA binding

Having established the antitumor properties of metal compounds **1a** and **1a'**, we then set out to study their interactions with DNA as a potential cellular target, as DNA recognition might partially account for the observed biological activity. With this in mind, we have studied DNA binding by using equilibrium dialysis, fluorescence-based DNA melting experiments and DNA viscometric titrations.

Dialysis experiments, based on the fundamental thermodynamic principle of equilibrium dialysis [71,87], were performed to determine apparent binding constants between DNA and the metal compounds. As the DNA targets, we selected CT DNA and a short oligonucleotide duplex of known sequence (ds17,17 bp).

The results obtained for compounds **1a** and **1a'** using two different DNA sequences are summarized in Table 2. Experiments were run based on adaptation of the protocol

described by Chaires [71], with some modifications as described in the Experimental section.

TABLE 2

Table 2 shows that these compounds have a modest to good binding affinity for duplex DNA, with apparent association constants in the order of 10^4 M^{-1}. In general, no significant differences in DNA affinity were found between the two enantiomers, although **1a** showed a two-fold better binding affinity in the case of CT DNA, whereas **1a'** displayed a better affinity towards the particular sequence of oligonucleotide ds17.

As part of our study on DNA interactions we were interested in determining the effect that these compounds may exert on the DNA denaturing temperature, Tm. We utilized a variable-temperature (FRET-melting) assay, an experiment that reduces DNA consumption while assessing a wide range of tested compound concentrations, it can be adapted to a high-throughput fashion, and it has been extensively used in the last years to determine the degree of thermal stabilization of different DNA structures in the presence of potential ligands [88]. Thus, FRET experiments were used to establish whether either the precursor ligands **a·HCl** and **a'·HCl** or the metal complexes **1a** and **1a'** were able to thermally stabilize duplex DNA structures.

In these experiments, a 10-bp oligonucleotide (F10T) labeled with two fluorophores, FAM at its 5' end and TAMRA at the 3' end, was selected [89]. If the metal complex binds to DNA affecting the stability of the helix, changes in the value of DNA Tm should be expected. Stabilization of duplex DNA usually results in increased values of Tm.

Metal complexes **1a** and **1a'** were analysed for their ability to affect duplex DNA melting in the 1-10 μM concentration range. However, under these conditions, these complexes did not produce a significant change in the DNA melting temperature

(ΔTm= -2 ºC at 10 μM, Fig S16). Furthermore, none of the enantiomers of the precursor ligands, **a·HCl** or **a'·HCl**, showed DNA stabilization. These results are in good agreement with previous reported DNA melting experiments on CT DNA with the metal compound **1a** [61] and seem to suggest that the compounds may interact with DNA in an external, mainly electrostatic fashion or through partial recognition of the DNA grooves.

Finally, DNA viscometric titrations were carried out as it is well known that viscosity measurements can provide a simple way to discriminate between the different binding modes of potential DNA ligands (especially non-covalent, such as intercalation *versus* groove or external binding) [90]. According to the theory of Cohen and Eisenberg [91], from gradual titration of DNA solutions with the compounds of interest, linear plots of the cubed root of the relative DNA viscosity $(\eta/\eta_o)^{1/3}$ versus the molar ratio of bound ligand to DNA nucleotide (r) can be obtained. The slope values in these plots correlate well with the DNA-ligand binding modes. Groove binding compounds normally display a slope close to 0.0, whereas classical mono-intercalants result in a slope close to 1.0 [90,91]. Experimentally, the slopes associated with prototype minor-groove binders, such as pentamidine, range from -0.3 to 0.2 [92], while those of classical mono-intercalators, such ethidium bromide, can vary from 0.80 to 1.50 [92-94].

Complexes **1a** and **1a'** showed a linear $(\eta/\eta_o)^{1/3}$ versus r correlation in the typical r range used in these experiments (Fig. 6) and produced some modification of the viscosity of the DNA solution at increasing concentrations, with negative slope values of -0.36 in the case of the enantiomer **1a** and -0.38 for the **1a'** counterpart.

FIGURE 6

It is evident from these results that these metal complexes do not interact with double stranded DNA by inserting the aromatic ring between the base pairs, thus a classical

intercalating interaction can be directly ruled out. This is no surprising taking into account the relative small surface of the arene ring. The viscosity slope values fall within or are close to the experimental values of typical groove binding ligands, but the negative slope may be also suggestive of a slight shortening of the DNA double helix, producing an overall effect of DNA compaction. It is known that metal complexes that bind DNA by a partial or non-classical intercalation (binding in the grooves or in the sugar-phosphate backbone) may decrease the DNA contour length by bending or kinking the DNA helix [95-97]. Although further studies should be carried out to determine the precise nature of this DNA interaction, these experiments suggest that DNA could act as a potential cellular target for these metal complexes and their interaction might partially contribute to the observed biological effect.

3.4. *In vivo* analysis

3.4.1. Effect of treatment of PC-3 cells with compound **1a** on the growth of xenografted PC-3 human prostate cancer cells

PC-3 cells were incubated in the absence or presence of **1a** for 24 h and then injected subcutaneously into the right flank of nude mice. Ten animals were used per group. Final tumor volume measurements revealed that the tumor growth was significantly inhibited by 45% (1,719 ± 206 mm^3) in **1a** group after 43 days, as compared with those from control group which measured 961 ± 160 mm^3 (Fig. S17, Table 3). Furthermore, the mean tumor weight was significantly reduced to 1,008 ± 103 mg compared with that in the control group (1,633 ± 153 mg), corresponding to a decrease of about 39% (Table 3). The Tumour Doubling Time (TDT) in the **1a** group was extended and was significantly different ($P < 0.05$) from doubling times in the control group (Table 3).

TABLE 3

Metal compounds which have demonstrated to be effective in decreasing tumor growth in an in vivo assay of nude mice bearing PC-3 tumor xenografts are the water soluble analogue of oxaliplatin, [Pt(*S*,*S*-1,2-diaminocyclohexane)(phen)]$Cl_2 \cdot 1.5H_2O \cdot 0.5HCl$ [98] and the promising Tacke's compound Titanocene-Y (bis-[(*p*-methoxybenzyl)cyclopentadienyl]titanium(IV) dichloride) [99].

3.4.2. Effect of treatment of PC-3 cells with **1a** on the expression of the activity of metalloproteinases-9 and -2 and on the expression of VEGF of xenografted PC-3 human prostate cancer cells

A significant correlation between the expression of MMP-9, MMP-2, and VEGF has been observed in cell lines as well as in tissue specimens of prostate cancer [100,101]. Overactive MMPs contribute to an almost complete loss of the basement membrane proteins in most cancers including prostate carcinomas [102]. Moreover, it has been described that the invasion and the motility of prostate tumor cells were increased by MMP-2 and MMP-9 [103]. Several studies have shown that VEGF is closely correlated with neovascularization and prognosis in many solid tumors. Thus, an increased expression of VEGF in prostate cancer [104], as well as a positive correlation between VEGF and Gleason score, tumor grade, and microvessel density, has been observed [104-107]. The successful antimetastatic NAMI-A compound was found to inhibit angiogenesis induced by VEGF *in vivo* [108].

The activity of both gelatinases was assessed by zymography assays (Fig. 7A). Latent forms of MMP-9 (95 kDa) and MMP-2 (72 kDa) were detected. The densitometric analysis showed that the activities of the latent-MMP forms decreased significantly by 45-49% ($P < 0.001$) in the **1a** group as compared with the control group. In order to determine whether these tumors presented increased angiogenesis and its possible

variations, we checked $VEGF_{165}$ levels by an ELISA assay. $VEGF_{165}$ expression showed a significant decrease of 48% in **1a** group (Fig. 7B).

FIGURE 7

In this first approach of establishing the potential therapeutic role of the compound **1a**, we exposed such a complex to androgen-independent prostate cancer cells and observed that it could affect the molecular machinery leading to a decrease in the tumorigenic capability of cells to represent the more aggressive form of prostatic adenocarcinoma or castration-resistant prostate cancers. In addition, levels of crucial molecules in the invasive phenotype as the main pro-angiogenic factor and the metaloproteinases -9 and -2 are found decreased.

These results suggest that the efficacy of **1a** as potential chemotherapeutic should be further explored. Additional experiments to determine the intraperitoneal efficacy of **1a** on nude mice PC-3 xenografts has been scheduled for the near future.

4. Conclusions

The use of optically active amino-oxime ligands derived from natural products is a useful and inexpensive strategy to synthesize water soluble, enantiopure arene ruthenium compounds. The oxime-containing Ru(II) compounds evaluated, **1a** and **1a'**, have shown potent anticancer activities against a broad range of different cancer cell lines, with no significant differences between the two ruthenium enantiomers. Both compounds induced apoptotic cell death of A-549 cells while dose-dependent cell death mechanisms have been found in the Jurkat cell line. This last fact could be of interest in the treatment of apoptosis-resistant tumors that are commonly resistant to chemotherapy. Compound-DNA interactions have been investigated by a variety of techniques, leading to the conclusion that these metal complexes likely interact with

double stranded DNA by external electrostatic interactions and/or groove binding, while a classical intercalation into the double strand DNA can be ruled out. The efficacy of **1a** in a preliminary *in vivo* assay of PC-3 xenografts in nude mice resulted in a promising inhibition of tumor growth by 45%. Analysis of tumor tissue showed a significant decrease of $VEGF_{165}$ expression and of latent-MMP forms activities, proteins correlated with angiogenesis and invasion and motility of prostate tumor cells, respectively. These results, along with those described before regarding the ability of **1a** to affect the metastatic phenotye of PC-3 cells *in vitro*, makes this oxime containing ruthenium compound a valuable choice for further investigations.

Abbreviations

A-549	Human cervical carcinoma cell line
A-278	Human ovarian cancer cell line
ABB	Annexin Binding Buffer
APT	Attached Proton Test
Bn	benzyl
BPC grade	Biotechnology Performance Certified grade
Cisplatin	*cis*-$[PtCl_2(NH_3)_2]$
CD	Circular Dichroism
COSY	Correlation Spectroscopy
Cq	Quaternary carbon
CT	Calf Thymus

1	DMSO	dimethylsulfoxide
2	DMEM	Dulbecco´s Modified Eagle´s Medium
3	DNA	Deoxyribonucleic acid
4	EDTA	ethylendiaminetetraacetic acid
5	ELISA	Enzyme-Linked Immuno Sorbent Assay
6	FAM	6-carboxyfluorescein
7	FBS	Fetal Bovine Serum
8	FRET	Fluorescence Resonance Energy Transfer
9	FT	Fourier Transform
10	F10T	5'-FAM-AGC TAT TA TA /sp18/ TA TA GCT ATA-TAMRA-3'
11	HCT-116	Human colorectal carcinoma cell line
12	HeLa	Human cervical cancer cell line
13	HSQC	Heteronuclear Single Quantum Coherence spectroscopy
14	HMBC	Heteronuclear Multiple Bond Correlation spectroscopy
15	HPLC	High Performance Liquid Chromatography
16	IDT	Integrated DNA Technologies
17	IR	Infrared
18	Jurkat	Human leukemic cancer cell line

Jurkat-pLVTHM	Human leukemic cancer cell line obtained by transfection with nonspecific short hairpin ribonucleic acid
Jurkat-shBak	Human leukemic cancer cell line obtained by ribonucleic acid interference of Bak
MIA PaCa-2	Human Pancreas Carcinoma cell line
MMP-2	metaloproteinase-2
MMP-9	metaloproteinase-9
MTT	3-(4,5-dimethylthiazol-2-yl)-2,5-diphenyltetrazolium bromide
NMR	Nuclear magnetic resonance
Oxaliplatin	[Pt(oxalate)(*R*,*R*-1,2-diaminocyclohexane)]
PAGE	PolyAcrylamide Gel Electrophoresis
PBS	Phosphate buffered saline solution
PC-3	Human androgen-independent prostate cancer cell line
RM175	$[(\eta^6\text{-}C_6H_5Ph)Ru(ethylendiamine)Cl][PF_6]$
RNA	ribonucleic acid
RNAi	ribonucleic acid interference
RPMI	Roswell Park Memorial Institute
SDS	Sodium Dodecyl Sulfate
shRNA	short hairpin ribonucleic acid

TAMRA Carboxytetramethylrhodamine.

TDT Tumour Doubling Time

Tm melting temperature

TM34 $[(\eta^5\text{-}C_5H_5)Ru(bypy)(PPh_3)][CF_3SO_3]$

Titanocene-Y bis-[(*p*-methoxybenzyl)cyclopentadienyl]titanium(IV) dichloride

UV-vis ultraviolet-visible

VEGF Vascular Endothelial Growth Factor

Acknowledgments

Financial support from Ministerio de Economía y Competitividad (MICINN CTQ2014-58270-R), Comunidad Autónoma de Madrid (CAM, I3 Program) and the Universidad de Alcalá (UAH, Projects CCG2015/EXP-082, CCG2015/BIO-010, CCG2016/EXP-044 and CCG2016/EXP-028) is acknowledged. I.C.A., S.S. and L.M.M. are grateful to UAH for their FPI-UAH fellowships.

Appendix A. Supplementary data. Supplementary data associated with this article can be found in the online version, at http://. These data include: Representative NMR, UV-vis and CD spectra of compounds **a·HCl**, **a'·HCl**, **1a, 1a'**. Elemental analysis data of **1a**. Selected biological data. Selected crystallographic data and bond lengths and angles for X-ray molecular structures of **1a'**.

[1] J. Reedijk, *Eur. J. Inorg. Chem. 2009* (2009) 1303-1312. DOI:10.1002/ejic.200900054.

[2] S. Medici, M. Peana, V. M. Nurchi, J. I. Lachowicz, G. Crisponi and M. A. Zoroddu, *Coord. Chem. Rev. 284* (2015) 329-350. DOI:10.1016/j.ccr.2014.08.002.

[3] C. Mari, V. Pierroz, S. Ferrari and G. Gasser, *Chem. Sci. 6* (2015) 2660-2686. DOI:10.1039/c4sc03759f.

[4] A. Bergamo and G. Sava, *Chem. Soc. Rev. 44* (2015) 8818-8835. DOI:10.1039/c5cs00134j.

[5] T. C. Johnstone, K. Suntharalingam and S. J. Lippard, *Chem. Rev. 116* (2016) 3436-3486. DOI:10.1021/acs.chemrev.5b00597.

[6] G. Palermo, A. Magistrato, T. Riedel, T. von Erlach, C. A. Davey, P. J. Dyson and U. Rothlisberger, *ChemMedChem 11* (2016) 1199-1210. DOI:10.1002/cmdc.201500478.

[7] W. Zheng, Y. Zhao, Q. Luo, Y. Zhang, K. Wu and F. Y. Wang, *Curr. Top. Med. Chem. 17* (2017) 3084-3098. DOI:10.2174/1568026617666170707124126.

[8] E. Alessio, *Eur. J. Inorg. Chem.* (2017) 1549-1560. DOI:10.1002/ejic.201600986.

[9] M. Cini, T. D. Bradshaw and S. Woodward, *Chem. Soc. Rev. 46* (2017) 1040-1051. DOI:10.1039/c6cs00860g.

[10] M. A. Jakupec, M. Galanski, V. B. Arion, C. G. Hartinger and B. K. Keppler, *Dalton Trans.* (2008) 183-194. DOI:10.1039/b712656p.

[11] R. Trondl, P. Heffeter, C. R. Kowol, M. A. Jakupec, W. Berger and B. K. Keppler, *Chem. Sci. 5* (2014) 2925-2932. DOI:10.1039/c3sc53243g.

[12] A. Bergamo, T. Riedel, P. J. Dyson and G. Sava, *Invest. New Drugs 33* (2015) 53-63. DOI:10.1007/s10637-014-0175-5.

[13] A. Bergamo, C. Gaiddon, J. H. M. Schellens, J. H. Beijnen and G. Sava, *J. Inorg. Biochem. 106* (2012) 90-99. DOI:10.1016/j.jinorgbio.2011.09.030.

[14] A. Weiss, R. H. Berndsen, M. Dubois, C. Muller, R. Schibli, A. W. Griffioen, P. J. Dyson and P. Nowak-Sliwinska, *Chem. Sci. 5* (2014) 4742-4748. DOI:10.1039/c4sc01255k.

[15] B. S. Murray, M. V. Babak, C. G. Hartinger and P. J. Dyson, *Coord. Chem. Rev. 306* (2016) 86-114. DOI:https://doi.org/10.1016/j.ccr.2015.06.014.

[16] E. Francotte and W. Lindner, *Chirality in Drug Research*, Wiley VCH, Weinheim, (2006).

[17] C. M. Manna, G. Armony and E. Y. Tshuva, *Inorg. Chem. 50* (2011) 10284-10291. DOI:10.1021/ic201340m.

[18] S. Blanck, J. Maksimoska, J. Baumeister, K. Harms, R. Marmorstein and E. Meggers, *Angew. Chem.-Int. Ed. 51* (2012) 5244-5246. DOI:10.1002/anie.201108865.

[19] K. J. Kilpin, S. M. Cammack, C. M. Clavel and P. J. Dyson, *Dalton Trans. 42* (2013) 2008-2014. DOI:10.1039/c2dt32333h.

[20] Y. Fu, R. Soni, M. J. Romero, A. M. Pizarro, L. Salassa, G. J. Clarkson, J. M. Hearn, A. Habtemariam, M. Wills and P. J. Sadler, *Chem.-Eur. J. 19* (2013) 15199-15209. DOI:10.1002/chem.201302183.

[21] G. Natile and L. G. Marzilli, *Coord. Chem. Rev. 250* (2006) 1315-1331. DOI:10.1016/j.ccr.2005.12.004.

[22] M. G. Mendoza-Ferri, C. G. Hartinger, R. E. Eichinger, N. Stolyarova, K. Severin, M. A. Jakupec, A. A. Nazarov and B. K. Keppler, *Organometallics 27* (2008) 2405-2407. DOI:10.1021/om800207t.

[23] Y. Fu, A. Habtemariam, A. Basri, D. Braddick, G. J. Clarkson and P. J. Sadler, *Dalton Trans. 40* (2011) 10553-10562. DOI:10.1039/c1dt10937e.

[24] Y. Fu, M. J. Romero, A. Habtemariam, M. E. Snowden, L. J. Song, G. J. Clarkson, B. Qamar, A. M. Pizarro, P. R. Unwin and P. J. Sadler, *Chem. Sci. 3* (2012) 2485-2494. DOI:10.1039/c2sc20220d.

[25] W. Ginzinger, G. Muhlgassner, V. B. Arion, M. A. Jakupec, A. Roller, M. Galanski, M. Reithofer, W. Berger and B. K. Keppler, *J. Med. Chem. 55* (2012) 3398-3413. DOI:10.1021/jm3000906.

[26] A. Kurzwernhart, W. Kandioller, C. Bartel, S. Bachler, R. Trondl, G. Muhlgassner, M. A. Jakupec, V. B. Arion, D. Marko, B. K. Keppler and C. G. Hartinger, *Chem. Commun. 48* (2012) 4839-4841. DOI:10.1039/c2cc31040f.

[27] S. Y. Bi, A. D. Wang, C. F. Bi, Y. H. Fan, Y. Xiao, S. B. Liu and Q. Wang, *Inorg. Chem. Commun. 15* (2012) 167-171. DOI:10.1016/j.inoche.2011.10.016.

[28] S. Blanck, Y. Geisselbrecht, K. Kraling, S. Middel, T. Mietke, K. Harms, L. O. Essen and E. Meggers, *Dalton Trans. 41* (2012) 9337-9348. DOI:10.1039/c2dt30940h.

[29] S. Newcombe, M. Bobin, A. Shrikhande, C. Gallop, Y. Pace, H. Yong, R. Gates, S. Chaudhuri, M. Roe, E. Hoffmann and E. M. E. Viseux, *Org. Biomol. Chem. 11* (2013) 3255-3260. DOI:10.1039/c3ob27460h.

[30] D. Csokas, B. I. Karolyi, S. Bosze, I. Szabo, G. Bati, L. Drahos and A. Csampai, *J. Organomet. Chem. 750* (2014) 41-48. DOI:10.1016/j.jorganchem.2013.10.057.

[31] H. Glasner and E. Y. Tshuva, *Inorg. Chem. 53* (2014) 3170-3176. DOI:10.1021/ic500001j.

[32] M. Frik, J. Fernandez-Gallardo, O. Gonzalo, V. Mangas-Sanjuan, M. Gonzalez-Alvarez, A. S. del Valle, C. H. Hu, I. Gonzalez-Alvarez, M. Bermejo, I. Marzo and M. Contel, *J. Med. Chem. 58* (2015) 5825-5841. DOI:10.1021/acs.jmedchem.5b00427.

[33] F. Arnesano, A. Pannunzio, M. Coluccia and G. Natile, *Coord. Chem. Rev. 284* (2015) 286-297. DOI:10.1016/j.ccr.2014.07.016.

[34] S. Tabassum, A. Asim, R. A. Khan, F. Arjmand, D. Rajakumar, P. Balaji and M. A. Akbarsha, *RSC Adv. 5* (2015) 47439-47450. DOI:10.1039/c5ra07333b.

[35] A. Dobrova, S. Platzer, F. Bacher, M. N. M. Milunovic, A. Dobrov, G. Spengler, E. A. Enyedy, G. Novitchi and V. B. Arion, *Dalton Trans. 45* (2016) 13427-13439. DOI:10.1039/c6dt02784a.

[36] S. F. Xi, L. Y. Bao, J. G. Lin, Q. Z. Liu, L. Qiu, F. L. Zhang, Y. X. Wang, Z. D. Ding, K. Li and Z. G. Gu, *Chem. Commun. 52* (2016) 10261-10264. DOI:10.1039/c6cc05743h.

[37] K. S. M. Smalley, R. Contractor, N. K. Haass, A. N. Kulp, G. E. Atilla-Gokcumen, D. S. Williams, H. Bregman, K. T. Flaherty, M. S. Soengas, E. Meggers and M. Herlyn, *Cancer Res. 67* (2007) 209-217. DOI:10.1158/0008-5472.can-06-1538.

[38] J. Maksimoska, L. Feng, K. Harms, C. L. Yi, J. Kissil, R. Marmorstein and E. Meggers, *J. Am. Chem. Soc. 130* (2008) 15764-15765. DOI:10.1021/ja805555a.

[39] C. M. Manna, G. Armony and E. Y. Tshuva, *Chem.-Eur. J. 17* (2011) 14094-14103. DOI:10.1002/chem.201102017.

[40] C. M. Manna and E. Y. Tshuva, *Dalton Trans. 39* (2010) 1182-1184. DOI:10.1039/b920786b.

[41] E. Menendez-Pedregal, J. Diez, A. Manteca, J. Sanchez, A. C. Bento, R. Garcia-Navas, F. Mollinedo, M. P. Gamasa and E. Lastra, *Dalton Trans. 42* (2013) 13955-13967. DOI:10.1039/c3dt51160j.

[42] M. Miller and E. Y. Tshuva, *Eur. J. Inorg. Chem. 2014* (2014) 1485-1491. DOI:10.1002/ejic.201301463.

[43] X. Q. Zhou, Q. Sun, L. Jiang, S. T. Li, W. Gu, J. L. Tian, X. Liu and S. P. Yan, *Dalton Trans. 44* (2015) 9516-9527. DOI:10.1039/c5dt00931f.

[44] Z. F. Chen, Q. P. Qin, J. L. Qin, J. Zhou, Y. L. Li, N. Li, Y. C. Liu and H. Liang, *J. Med. Chem. 58* (2015) 4771-4789. DOI:10.1021/acs.jmedchem.5b00444.

[45] M. Cini, T. D. Bradshaw, S. Woodward and W. Lewis, *Angew. Chem.-Int. Ed. 54* (2015) 14179-14182. DOI:DOI: 10.1002/anie.201508034.

[46] M. Cini, H. Williams, M. W. Fay, M. S. Searle, S. Woodward and T. D. Bradshaw, *Metallomics 8* (2016) 286-297. DOI:10.1039/c5mt00297d.

[47] S. A. Abramkin, U. Jungwirth, S. M. Valiahdi, C. Dworak, L. Habala, K. Meelich, W. Berger, M. A. Jakupec, C. G. Hartinger, A. A. Nazarov, M. Galanski and B. K. Keppler, *J. Med. Chem. 53* (2010) 7356-7364. DOI:10.1021/jm100953c.

[48] Y. Fu, C. Sanchez-Cano, R. Soni, I. Romero-Canelon, J. M. Hearn, Z. Liu, M. Wills and P. J. Sadler, *Dalton Trans. 45* (2016) 8367-8378. DOI:10.1039/c6dt01242f.

[49] V. Y. Kukushkin and A. J. L. Pombeiro, *Coord. Chem. Rev. 181* (1999) 147-175 and references therein. DOI:10.1016/s0010-8545(98)00215-x.

[50] Y. Y. Scaffidi-Domianello, K. Meelich, M. A. Jakupec, V. B. Arion, V. Y. Kukushkin, M. Galanski and B. K. Keppler, *Inorg. Chem. 49* (2010) 5669-5678. DOI:10.1021/ic100584b.

[51] S. Soga, L. M. Neckers, T. W. Schulte, Y. Shiotsu, K. Akasaka, H. Narumi, T. Agatsuma, Y. Ikuina, C. Murakata, T. Tamaoki and S. Akinaga, *Cancer Res. 59* (1999) 2931-2938 (and references therein).

[52] C. Bartel, A. K. Bytzek, Y. Y. Scaffidi-Domianello, G. Grabmann, M. A. Jakupec, C. G. Hartinger, M. Galanski and B. K. Keppler, *J. Biol. Inorg. Chem. 17* (2012) 465-474. DOI:10.1007/s00775-011-0869-5.

[53] K. Ossipov, Y. Y. Scaffidi-Domianello, I. F. Seregina, M. Galanski, B. K. Keppler, A. R. Timerbaev and M. A. Bolshov, *J. Inorg. Biochem. 137* (2014) 40-45. DOI:10.1016/j.jinorgbio.2014.04.008.

[54] S. Wirth, C. J. Rohbogner, M. Cieslak, J. Kazmierczak-Baranska, S. Donevski, B. Nawrot and I. P. Lorenz, *J. Biol. Inorg. Chem. 15* (2010) 429-440. DOI:10.1007/s00775-009-0615-4.

[55] N. Chitrapriya, V. Mahalingam, M. Zeller, H. Lee and K. Natarajan, *J. Mol. Struct. 984* (2010) 30-38. DOI:10.1016/j.molstruc.2010.09.004.

[56] S. Adhikari, N. R. Palepu, D. Sutradhar, S. L. Shepherd, R. M. Phillips, W. Kaminsky, A. K. Chandra and M. R. Kollipara, *J. Organomet. Chem. 820* (2016) 70-81. DOI:10.1016/j.jorganchem.2016.08.004.

[57] N. Chitrapriya, V. Mahalingam, L. C. Channels, M. Zeller, F. R. Fronczek and K. Natarajan, *Inorg. Chim. Acta 361* (2008) 2841-2850. DOI:10.1016/j.ica.2008.02.010.

[58] G. Sava, G. Jaouen, E. A. Hillard and A. Bergamo, *Dalton Trans. 41* (2012) 8226-8234. DOI:10.1039/c2dt30075c.

[59] N. P. E. Barry and P. J. Sadler, *Chem. Commun. 49* (2013) 5106-5131. DOI:10.1039/c3cc41143e.

[60] H. Brunner, *Eur. J. Inorg. Chem.* (2001) 905-912. DOI:10.1002/1099-0682(200104)2001:4.

[61] Y. Benabdelouahab, L. Munoz-Moreno, M. Frik, I. de la Cueva-Alique, M. A. El Amrani, M. Contel, A. M. Bajo, T. Cuenca and E. Royo, *Eur. J. Inorg. Chem.* (2015) 2295-2307. DOI:10.1002/ejic.201500097.

[62] D. J. Brecknell, R. M. Carman, B. Singaram and J. Verghese, *Aust. J. Chem. 30* (1977) 195-203. DOI:10.1071/ch9770195.

[63] A. V. Tkachev, A. V. Rukavishnikov, A. M. Chibiryaev, A. Y. Denisov, Y. V. Gatilov and I. Y. Bagryanskaya, *Aust. J. Chem. 45* (1992) 1077-1086. DOI:10.1071/CH9921077.

[64] S. V. Larionov, *Russ. J. Coord. Chem. 38* (2012) 1-23 (and references therein). DOI:10.1134/s1070328412010058.

[65] M. S. I. El Alami, M. A. El Amrani, F. Agbossou-Niedercorn, I. Suisse and A. Mortreux, *Chem.-Eur. J. 21* (2015) 1398-1413. DOI:10.1002/chem.201404303.

[66] R. M. Carman, P. C. Mathew, G. N. Saraswathi, B. Singaram and J. Verghese, *Aust. J. Chem. 30* (1977) 1323-1335.

[67] M. S. Ibn El Alami, M. A. El Amrani, A. Dahdouh, P. Roussel, I. Suisse and A. Mortreux, *Chirality 24* (2012) 675-682. DOI:10.1002/chir.22073.

[68] G. E. Trenter in *Spectroscopic Analysis: Polarimetry and Optical Rotatory Dispersion*, *Vol. 8* Eds.: E. M. Carreira and H. Yamamoto), Elsevier, (2012) pp. 411-421.

[69] L. J. Farrugia, *J. Appl. Crystallogr. 45* (2012) 849-854. DOI:10.1107/s0021889812029111.

[70] G. M. Sheldrick, *Acta Crystallogr. Sect. A 71* (2015) 3-8. DOI:10.1107/s2053273314026370.

[71] J. B. Chaires in *Structural selectivity of drug-nucleic acid interactions probed by competition dialysis*, *Vol. 253* Eds.: M. J. Waring and J. B. Chaires), Springer-Verlag Berlin, Berlin, (2005) pp. 33-53.

[72] H. Brunner, R. Oeschey and B. Nuber, *Organometallics 15* (1996) 3616-3624. DOI:10.1021/om960215a.

[73] T. R. Ward, O. Schafer, C. Daul and P. Hofmann, *Organometallics 16* (1997) 3207-3215. DOI:10.1021/om9700369.

[74] J. W. Faller, B. P. Patel, M. A. Albrizzio and M. Curtis, *Organometallics 18* (1999) 3096-3104. DOI:10.1021/om981053g.

[75] R. Noyori and S. Hashiguchi, *Accounts Chem. Res. 30* (1997) 97-102. DOI:10.1021/ar9502341.

[76] A. Zelewsky, *Coord. Chem. Rev. 190-192* (1999) 811-825.

[77] I. Y. Shabalina, V. P. Kirin, V. A. Maksakov, A. V. Virovets, A. V. Golovin, A. M. Agafontsev and A. V. Tkachev, *Russ. J. Coord. Chem. 34* (2008) 286-294. DOI:10.1134/s1070328408040088.

[78] V. P. Kirin, I. Y. Prikhod'ko, V. A. Maksakov, A. V. Virovets, A. M. Agafontsev and B. A. Golovin, *Russ. Chem. Bull. 58* (2009) 1371-1382. DOI:10.1007/s11172-009-0183-3.

[79] G. Chahboun, J. A. Brito, B. Royo, M. A. El Amrani, E. Gomez-Bengoa, M. E. G. Mosquera, T. Cuenca and E. Royo, *Eur. J. Inorg. Chem.* (2012) 2940-2949. DOI:10.1002/ejic.201200144.

[80] S. K. Singh, S. Sharma, S. D. Dwivedi, R. Q. Zou, Q. Xu and D. S. Pandey, *Inorg. Chem. 47* (2008) 11942-11949. DOI:10.1021/ic8009699.

[81] M. Frik, A. Martinez, B. T. Elie, O. Gonzalo, D. R. de Mingo, M. Sanau, R. Sanchez-Delgado, T. Sadhukha, S. Prabha, J. W. Ramos, I. Marzo and M. Contel, *J. Med. Chem. 57* (2014) 9995-10012. DOI:10.1021/jm5012337.

[82] R. L. Hayward, Q. C. Schornagel, R. Tente, J. C. Macpherson, R. E. Aird, S. Guichard, A. Habtemariam, P. Sadler and D. I. Jodrell, *Cancer Chemother. Pharmacol. 55* (2005) 577-583. DOI:10.1007/s00280-004-0932-9.

[83] P. R. Florindo, D. M. Pereira, P. M. Borralho, C. M. P. Rodrigues, M. F. M. Piedade and A. C. Fernandes, *J. Med. Chem. 58* (2015) 4339-4347. DOI:10.1021/acs.jmedchem.5b00403.

[84] Z. Ude, I. Romero-Canelón, B. Twamley, D. Fitzgerald Hughes, P. J. Sadler and C. J. Marmion, *J. Inorg. Biochem. 160* (2016) 210-217. DOI:https://doi.org/10.1016/j.jinorgbio.2016.02.018.

[85] A. I. Tomaz, T. Jakusch, T. S. Morais, F. Marques, R. F. M. de Almeida, F. Mendes, E. A. Enyedy, I. Santos, J. C. Pessoa, T. Kiss and M. H. Garcia, *J. Inorg. Biochem. 117* (2012) 261-269. DOI:10.1016/j.jinorgbio.2012.06.016.

[86] N. Lopez-Royuela, P. Perez-Galan, P. Galan-Malo, V. J. Yuste, A. Anel, S. A. Susin, J. Naval and I. Marzo, *Biochem. Pharmacol. 79* (2010) 1746-1758. DOI:10.1016/j.bcp.2010.02.010.

[87] W. Muller and D. M. Crothers, *Eur. J. Biochem. 54* (1975) 267-277. DOI:10.1111/j.1432-1033.1975.tb04137.x.

[88] D. Renciuk, J. Zhou, L. Beaurepaire, A. Guedin, A. Bourdoncle and J. L. Mergny, *Methods 57* (2012) 122-128. DOI:10.1016/j.ymeth.2012.03.020.

[89] R. Kieltyka, P. Englebienne, J. Fakhoury, C. Autexier, N. Moitessier and H. F. Sleiman, *J. Am. Chem. Soc. 130* (2008) 10040-+. DOI:10.1021/ja8014023.

[90] D. Suh and J. B. Chaires, *Bioorg. Med. Chem. 3* (1995) 723-728. DOI:10.1016/0968-0896(95)00053-j.

[91] G. Cohen and H. Eisenberg, *Biopolymers 8* (1969) 45-+. DOI:10.1002/bip.1969.360080105.

[92] T. A. Fairley, R. R. Tidwell, I. Donkor, N. A. Naiman, K. A. Ohemeng, R. J. Lombardy, J. A. Bentley and M. Cory, *J. Med. Chem. 36* (1993) 1746-1753. DOI:10.1021/jm00064a008.

[93] D. S. Drummond, N. J. Pritchard, Simpsong.Vf and A. R. Peacocke, *Biopolymers 4* (1966) 971-+. DOI:10.1002/bip.1966.360040903.

[94] Y. Kubota, K. Hashimoto, K. Fujita, M. Wakita, E. Miyanohana and Y. Fujisaki, *478* (1977) 23-32. DOI:10.1016/0005-2787(77)90240-4.

[95] T. Topala, A. Bodoki, L. Oprean and R. Oprean, *Farmacia 62* (2014) 1049-1061.

[96] N. Sohrabi, N. Rasouli and M. Kamkar, *Bull. Korean Chem. Soc. 35* (2014) 2523-2528. DOI:10.5012/bkcs.2014.35.8.2523.

[97] G. Yang, J. Z. Wu, L. Wang, L. N. Ji and X. Tian, *J. Inorg. Biochem. 66* (1997) 141-144. DOI:10.1016/s0162-0134(96)00194-8.

[98] D. M. Fisher, R. R. Fenton and J. R. Aldrich-Wright, *Chem. Commun.* (2008) 5613-5615. DOI:10.1039/b811723c.

[99] C. M. Dowling, J. Claffey, S. Cuffe, I. Fichtner, C. Pampillon, N. J. Sweeney, K. Strohfeldt, R. W. G. Watson and M. Tacke, *Lett. Drug Des. Discov. 5* (2008) 141-144. DOI:10.2174/157018008783928463.

[100]R. Aalinkeel, M. P. N. Nair, G. Sufrin, S. A. Mahajan, K. C. Chadha, R. P. Chawda and S. A. Schwartz, *Cancer Res. 64* (2004) 5311-5321. DOI:10.1158/0008-5472.can-2506-2.

[101]B. Wegiel, A. Bjartell, J. Tuomela, N. Dizeyi, M. Tinzl, L. Helczynski, E. Nilsson, L. E. Otterbein, P. Harkonen and J. L. Persson, *J. Natl. Cancer Inst. 100* (2008) 1022-1036. DOI:10.1093/jnci/djn214.

[102]Y. G. Zhao, A. Z. Xiao, R. G. Newcomer, H. I. Park, T. B. Kang, L. W. K. Chung, M. G. Swanson, H. E. Zhau, J. Kurhanewicz and Q. X. A. Sang, *J. Biol. Chem. 278* (2003) 15056-15064. DOI:10.1074/jbc.M210975200.

[103]M. Iiizumi, S. Bandyopadhyay, S. K. Pai, M. Watabe, S. Hirota, S. Hosobe, T. Tsukada, K. Miura, K. Saito, E. Furuta, W. Liu, F. Xing, H. Okuda, A. Kobayashi and K. Watabe, *Cancer Res. 68* (2008) 7613-7620. DOI:10.1158/0008-5472.can-07-6700.

[104]D. Stefanou, A. Batistatou, S. Kamina, E. Arkoumani, D. J. Papachristou and N. J. Agnantis, *In Vivo 18* (2004) 155-160.

[105]G. Kaygusuz, O. Tulunay, S. Baltaci and O. Gogus, *Int. Urol. Nephrol. 39* (2007) 841-850. DOI:10.1007/s11255-006-9144-z.

[106]R. Mori, T. B. Dorff, S. G. Xiong, C. J. Tarabolous, W. Ye, S. Groshen, K. D. Danenberg, P. V. Danenberg and J. K. Pinski, *Prostate 70* (2010) 1692-1700. DOI:10.1002/pros.21204.

[107]D. Strohmeyer, F. Strauss, C. Rossing, C. Roberts, O. Kaufmann, G. Bartsch and P. Effert, *Anticancer Res. 24* (2004) 1797-1804.

[108]L. Morbidelli, S. Donnini, S. Filippi, L. Messori, F. Piccioli, P. Orioli, G. Sava and M. Ziche, *Br. J. Cancer 88* (2003) 1484-1491. DOI:10.1038/sj.bjc.6600906.

[109]J. Fernandez-Gallardo, B. T. Elie, F. J. Sulzmaier, M. Sanau, J. W. Ramos and M. Contel, *Organometallics 33* (2014) 6669-6681. DOI:10.1021/om500965k.

[110]F. W. Liu, R. Anis, E. M. Hwang, R. Ovalle, A. Varela-Ramirez, R. J. Aguilera and M. Contel, *Molecules 16* (2011) 6701-6720. DOI:10.3390/molecules16086701.

Figures and Tables

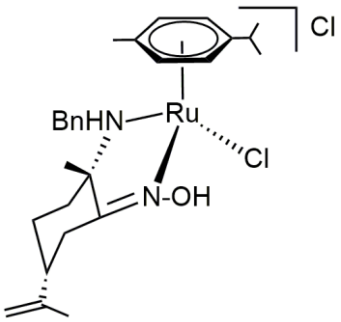

1a (R_{Ru}, R_N,*1S,4R*)

Fig. 1. Optically active ruthenium compound containing an amino-oxime ligand derived from *R*-limonene.

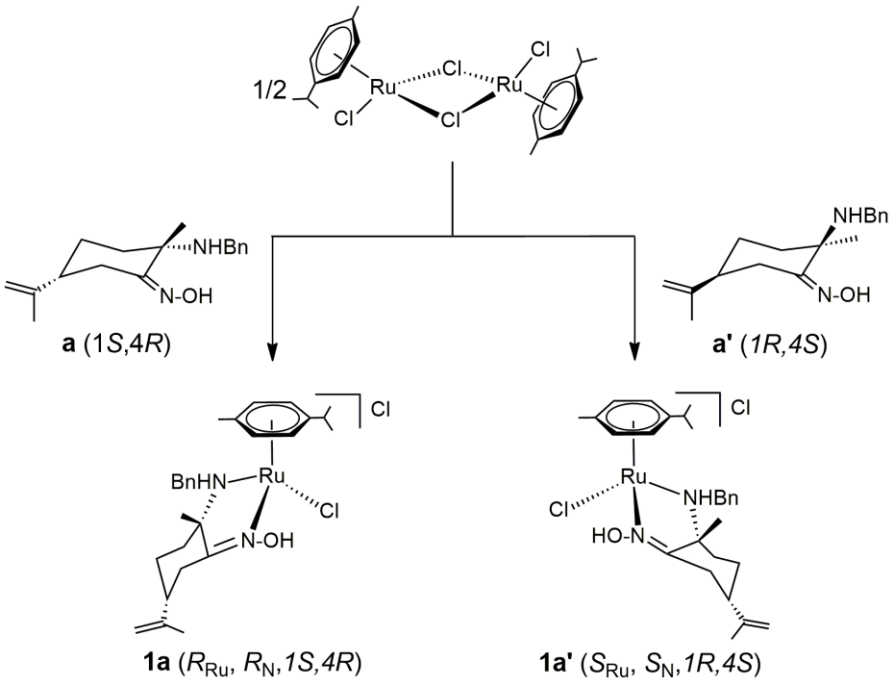

a (1*S*,4*R*) **a'** (*1R,4S*)

1a (R_{Ru}, R_N,*1S,4R*) **1a'** (S_{Ru}, S_N,*1R,4S*)

Fig. 2. Synthesis of optically active amino-oxime ruthenium compounds.

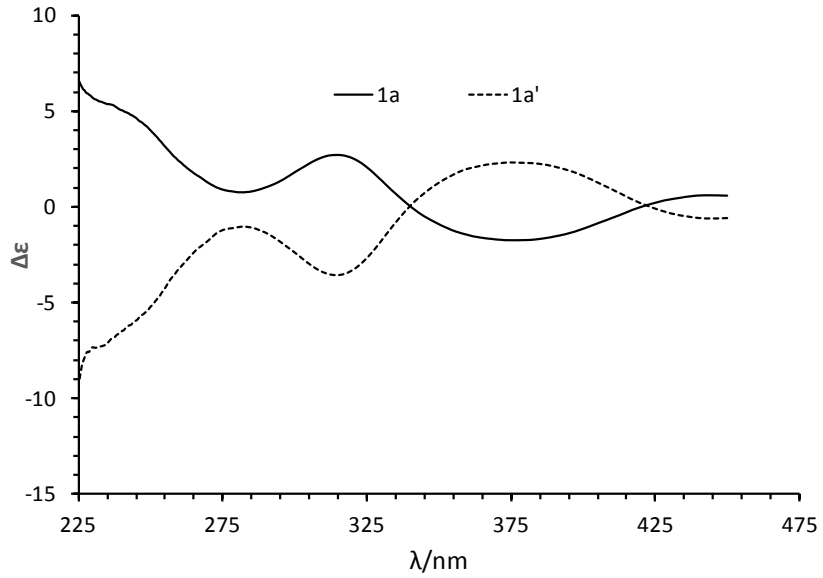

Fig. 3. The CD spectra of enantiomers **1a** and **1a'** in water solution.

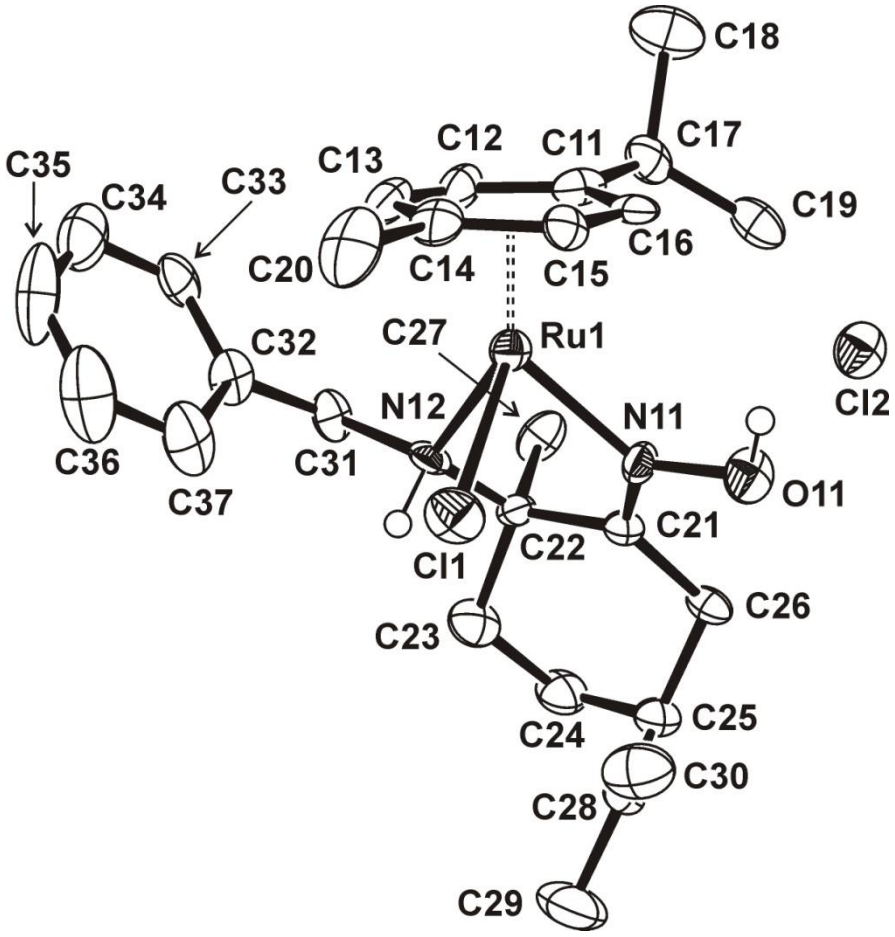

Fig. 4. ORTEP drawing of compound **1a'** with 50% probability ellipsoids. Hydrogen bonded to carbon atoms have been omitted for clarity. Representative lengths (Å) and angles (deg): Ru(1)-Ct(1) 1.674; Ru(1)-Cl(1) 2.404(4); Ru(1)-N(11) 2.067(10); Ru(1)-N(12) 2.173(10); N(11)-O(11) 1.381(13); Cl(1)-Ru(1)-N(11) 82.9(3); Cl(1)-Ru(1)-N(12) 81.8(3); N(11)-Ru(1)-N(12) 75.8(4); Ru(1)-N(11)-O(11) 124.0(8); Ru(1)-N(11)-C(21) 121.6(8); O(11)-N(11)-C(21) 114.4(10); Ru(1)-N(12)-C(22) 111.1(7); Ru(1)-N(12)-C(31) 120.6(8); C(22)-N(12)-C(31) 112.7(10); (Ct(1) is the centroid of the C(11)-C(16) ring).

Table 1. IC_{50} values (μM) of metal compounds **1a** and **1a'** in a variety of human cell lines.[a,b]

	Metal compounds		
	1a	**1a'**	Cisplatin
PC-3	8.70 ± 1.50	14.0 ± 2.4	104.2 ± 8.1
A-549	7.2 ± 1.5	9.1 ± 2.4	114.2 ± 9.1[b]
MIA PaCa-2	9.7 ± 2.1	13.1 ± 2.6	76.5 ± 7.4[b]
HCT-116	11.5 ± 2 .0	18.4 ± 1.8	34.9 ± 3.0[b]
Jurkat-T	4.0 ± 0.7	4.7 ± 0.9	10.8 ± 1.2[b]
HeLa	7.5 ± 1.2	6.7 ± 1.4	--

[a] Data are expressed as mean ± S.D. (n = 4)

[b] Values obtained with the same technique, cell lines and incubation times [32,45,81,109,110].

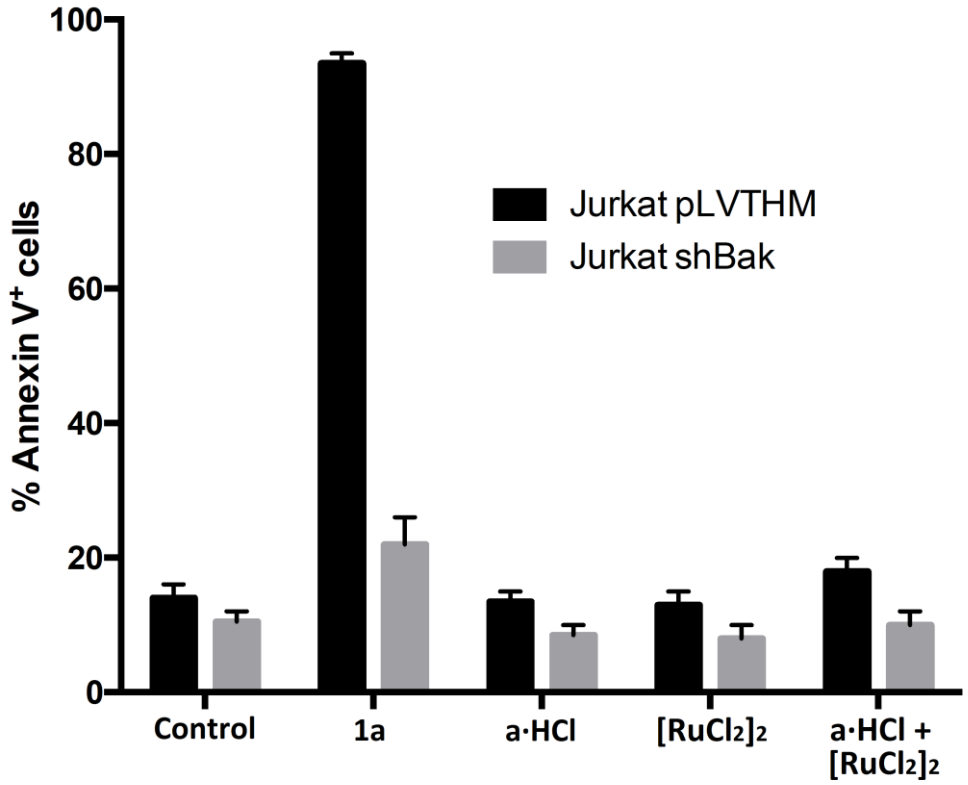

Fig. 5. Comparison of the effect of $[(\eta^6\text{-}p\text{-cymene})RuCl_2]_2$ + **a·HCl**, **a·HCl** and **1a** on Jurkat-T cell apoptosis after 24 h of exposure ($[RuCl_2]_2 = [(\eta^6\text{-}p\text{-cymene})RuCl_2]_2$).

Table 2. DNA apparent association constants of ruthenium(II) compounds obtained by equilibrium dialysis[(a)].

	Compound 1a	**Compound 1a'**
DNA	K_{app} (M^{-1}) $\times 10^{-4}$	$K_{app} \times 10^{-4}$
Calf Thymus (CT)	3.0 ± 0.3	1.5 ± 0.2
ds17 sequence	2.4 ± 0.2	7.9 ± 0.3

[a] Metal complex solutions were equilibrated with 75 μM of nucleic acid (in each dialysis bag) for 24 h at room temperature. UV-visible spectra were recorded after detergent addition and the concentrations of free and DNA-bound ligands determined. The competition dialysis data were used to calculate the 1a and 1a' apparent association constants, given by the equation Kapp = Cb/(Cf)(Stotal-Cb), where Cb is the amount of metal complex bound, Cf is the free metal complex concentration and Stotal = 75 μM, in monomeric units.

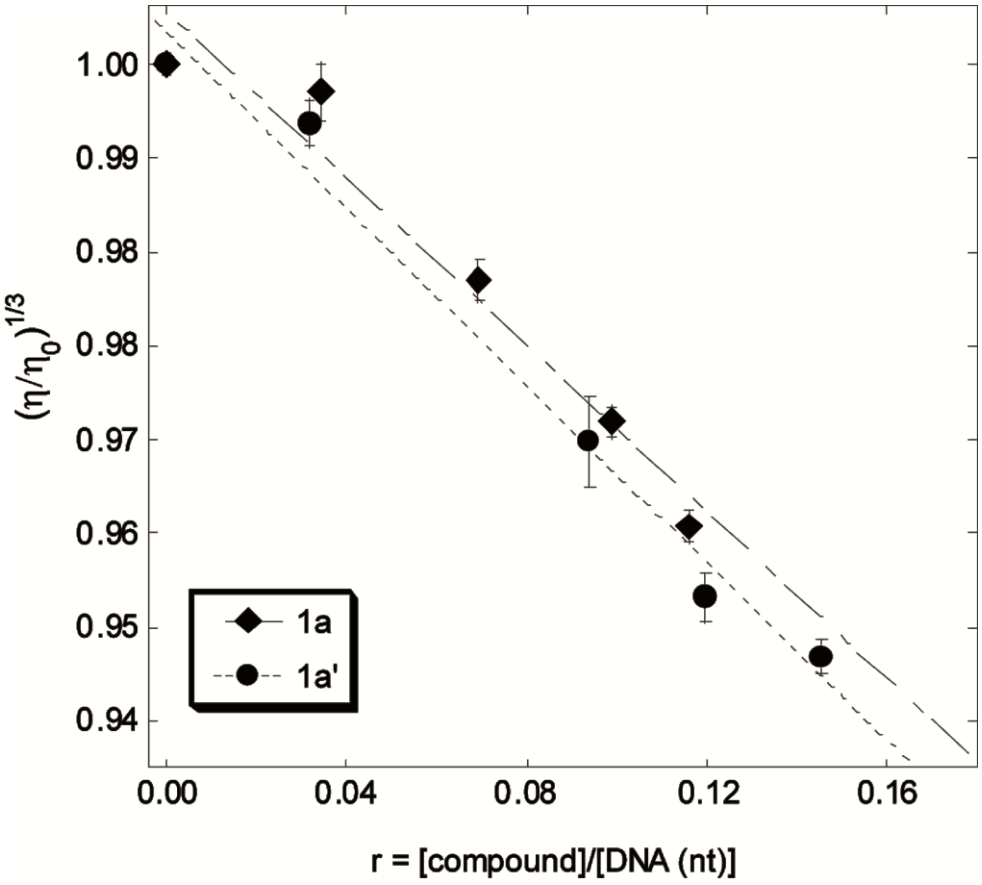

Fig. 6. Viscometric titrations of *Calf Thymus* (CT) DNA and metal complexes **1a** and **1a'**, at 25 ºC (10 mM sodium phosphate buffer, pH 7.2).

Table 3. Effect of treatment of PC-3 cells with **1a** on tumor weight, tumor burden and Tumor Doubling Time (TDT). Values are mean ± SE. *, $P < 0.05$ *vs*. control group.

Groups	**Tumor weight, mg (% inhibition)**	**Tumor burden, mg/g body weight (% inhibition)**	**TDT, days (% increase)**
Control (n = 10)[a]	1,633.8 ± 153	53.4 ± 5.6	8.68 ± 0.52
1a (n = 10)[a]	1,008 ± 103 (39)*	36.6 ± 3.1 (68)*	10.84 ± 0.58 (25)*

[a] (number of animals)

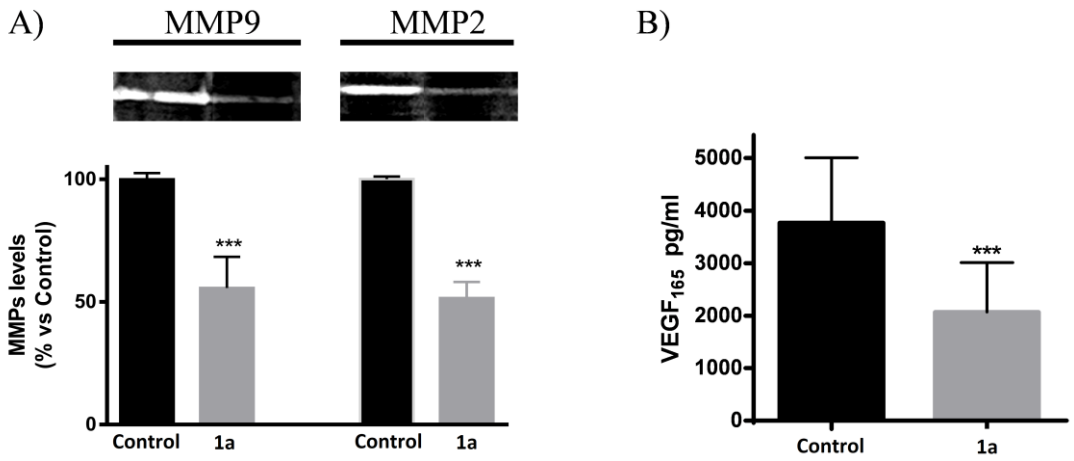

Fig. 7. Effect of treatment of PC-3 cells with compound **1a** on A) the activity of metaloproteinase 9 and 2, and B) the expression of the proangiogenic factor $VEGF_{165}$. Androgen-independent prostate cancer cells were incubated in the absence or presence of **1a** (2.5 μM) for 24 h. The cell suspension was mixed with Matrigel® and injected subcutaneously into the right flank of nude mice ($5x10^6$ cells/mouse). Ten mice were used in each group. Pro-MMPs activities, as well as $VEGF_{165}$ levels, were determined in tumor homogenates (25 μg) by ELISA and gelatin zymography. Data in each bar are the means ± SE. ***, $P < 0.001$ *vs*. control group.